Defect and Diffusion Forum
ISSN: 1662-9507, Vol. 426, pp 51-56
doi:10.4028/p-di3si0

Submitted: 2022-09-04
Revised: 2022-11-21
Accepted: 2022-11-25
Online: 2023-06-06

Analysis of Strain in Ion Implanted 4H-SiC by Fringes Observed in Synchrotron X-Ray Topography

Zeyu Chen[1,a*], Yafei Liu[1,b], Hongyu Peng[1,c], Qianyu Cheng[1,d], Shanshan Hu[1,e], Balaji Raghothamachar[1,f], Michael Dudley[1,g], Reza Ghandi[2,h], Stacey Kennerly[2,i], and Peter Thieberger[3,j]

[1]Department of Materials Science & Chemical Engineering, Stony Brook University, Stony Brook, NY 11794 USA

[2]GE Research, Niskayuna, NY, 12309, USA

[3]Brookhaven National Laboratory, Upton, NY, 11973, USA

[a]Zeyu.chen@stonybrook.edu, [b]Yafei.liu@stonybrook.edu, [c]Hongyu.peng@stonybrook.edu, [d]Qianyu.cheng@stonybrook.edu, [e]Shanshan.Hu@stonybrook.edu, [f]Balaji.raghothamachar@stonybrook.edu, [g]Michael.dudley@stonybrook.edu, [h]Ghandi@ge.com, [i]Stacey.kennerly@ge.com, [j]Thieber@bnl.com

Keywords: 4H-SiC, Ion Implantation, Lattice Strain, Synchrotron X-ray Plane Wave Topography

Abstract. A novel high energy implantation system has been successfully developed to fabricate 4H-SiC superjunction devices for medium and high voltage via implantation of dopant atoms with multi-energy ranging from 13 to 66 MeV. Level of energy used is significantly higher than that of conventional implantation, so lattice damage caused by such implantation must be characterized in detail to enhance the understanding of the nature of the damage. In regard to this, by employing the novel high energy system, 4H-SiC wafer with 12 μm epilayer was blanket implanted by 13.8 to 65.7 MeV Al atoms and energy range up to 42.99 MeV N atoms. The lattice damages induced by the implantation were primarily characterized by Synchrotron X-ray Topography. Multiple asymmetric diffraction peaks with an angular separation of only 2" (arcseconds) were shown in the topographs, indicating inhomogeneous strain distribution across the implanted layer. The strain profile of the implanted layer was obtained by Rocking-curve Analysis by Dynamical Simulation (RADS).

Introduction

Silicon Carbide (SiC) is a promising wide bandgap semiconductor for power devices. Due to the excellent properties of SiC, such as wide band gap, high break down voltage and thermal stability, SiC devices are able to be operated under harsh environment, such as high temperature, high voltage and high frequency environment [1]. 4H-SiC high voltage devices, which can withstand 1.7 to 6.5 kV, are highly sought for applications, such as hybrid aircraft, shipboard and power grid systems, and high-speed trains. Usually, such medium or high voltage devices are fabricated on 4H-SiC wafers with thick epilayers that can increase the breakdown of the device [2]. However, doping such thick epilayers is quite challenging. An optimized solution of selective area doping is utilizing multi-steps high energy ion implantation system. Such a system has been developed at the Tandem Van de Graaff accelerator facility at Brookhaven National Laboratory with the capability of multi-steps high energy implantation at energies up to 150 MeV [3]. By employing such a system, medium voltage charge balance devices and 2 kV superjunction structure PIN diode have been demonstrated [6,7]. Implantation employing high energy ions can create lattice strain in the epilayer by displacing the host atoms. Such lattice strain is usually recovered during activation annealing but any residual damage can still impact the performance of the SiC devices. Therefore, characterization of strain in as-implanted epilayer is critical to understand the nature of damage introduced by the high energy implantation.

Synchrotron X-ray plane wave topography (SXPWT) [8], (previously referred as synchrotron X-ray rocking curve topography (SXRCT) [9,10,11]), is capable of measuring strain and tilt of 4H-SiC with a strain sensitivity of the order of 10^{-6}. Wieteska, Wierzchowski and coworkers have observed

various peaks and fringes in implanted Si and $Al_xGa_{1-x}As$/GaAs epilayer by SXPWT, which show same angular positions as synchrotron rocking curve with double crystal monochromator [12,13]. In this study, we employ SXPWT and Rocking-curve Analysis by Dynamical Simulation (RADS) to conduct a detailed study and explore the extent and nature of the strain in 4H-SiC introduced by high energy ion implantation by Al ions. Here, we reported fringes showing in SXPWT to emphasize the importance of the curve width of the probe and the information gained from the fringes of SXPWT.

Experiment

For the present experiment, 4H-SiC with 12 μm of epilayer was blanket multi-step high energy implanted with both Al and N atoms without annealing process and a box concentration profile was created. The implantation was carried out at the Tandem Van de Graaff facility at Brookhaven National Laboratory (BNL) [3]. Due to the difference in atomic mass bettween the two dopant atoms, energy ranges used were different to achieve implant depth of 12 μm. Energy range of 13.8 to 65.7 MeV were used for Al implantation, while N atoms were implanted at energies ranging up to 42.99 MeV. The fluence of implantation with each dopant atoms is 5.56 x 10^{13} cm^{-2}. The implanted wafer was charaterized by SXPWT with double crystal setup, as shown in Fig. 1, where Si(331) beam conditioner, following the Si(111) double crystal monochromator, acts as the first crystal and 4H-SiC in (0008) reflection is the second one. To image the whole sample, the wafer was rotate about $[1\bar{1}00]$ direction in steps of 4 microradians (0.825 arcseconds). A strain map processed by MATLAB program[4,5], was obtained by recording two series of images in 0° and 180° positions about the normal of the (0008) plane. The topographs were recorded by a CCD camera with pixel size of 2.5 μm.

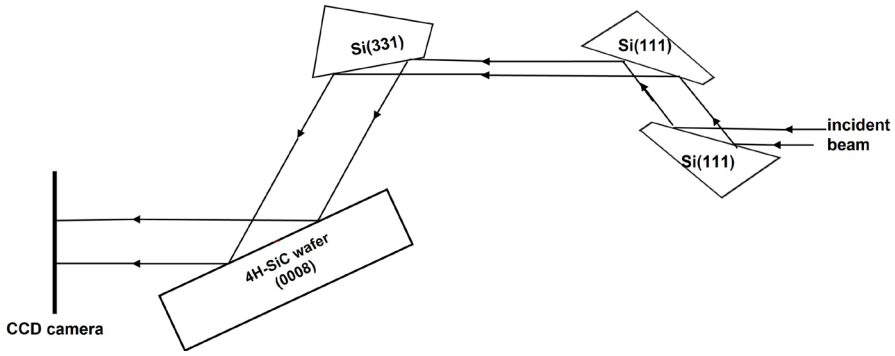

Figure 1. Schematic of experimental setup of SXPWT, where Si(331) beam conditioner was used in between the Si(111) monochromator and 4H-SiC sample. CCD camera was used to collect the topograph images.

Discussion

Fringe pattern and satellite peak analysis have been widely used for characterizing the strain gradient in the ion implanted materials [11,14]. If the separation of the fringes is approximated wider than 10", the conventional high-resolution X-ray diffractometry with monochromator can reveal such patterns. Here, we recorded fringes with separation about 2" that can only be revealed from SWPXT since the 0.5" width of the incident beam (determined from DuMond diagrams) can be provided by the asymmetric Si (331) beam conditioner, which acts as an extremely fine probe [8]. With such a fine probe, SWPXT is highly sensitive to lattice distortion. Fig.2 shows optical picture and individual image of topographs illustrating the contour recorded from the CCD camera, where the intensity profile of the contour on topograph can be treated as a rocking curve. Normally, the topograph will show contour consisting of one peak. However, in the case of the topograph of the implanted wafer, contour can be observed in Fig. 2, including two peaks with higher intensities and fringes with relatively weak intensities. Unimplanted region is highlighted by the red dash line to compare with the two peaks, where only the top peak is continuous with the diffracted peak in the unimplanted region, indicating that the top peak is diffracted from the substrate having the same undisturbed

structure as the unimplanted region since the whole epilayer was implanted. Therefore, such peak is denoted as the main peak and the peak with relatively high intensity at the bottom is denoted as the satellite peak. According to dynamical theory of X-ray diffraction [15], a constant strain will result in a rocking curve with symmetric fringes and satellite peak, while fringes and satellite peak are lying on one side of the main peak, illustrating that the strain gradient exist in the implanted layer.

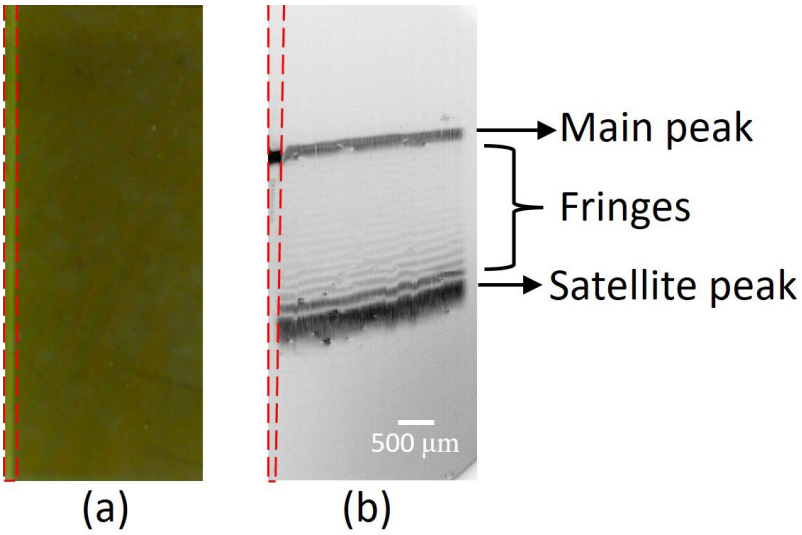

Figure 2. (a) Optical image showing implanted and unimplanted (enclosed in red dash lines) (b) Individual contour image of topograph at a single angular position where the main peak (substrate/unimplanted epilayer) and satellite peak (implanted epilayer) are indicated by the dark arrows, and the intermediary fringes are indicated by the right brace. Note that the unimplanted region highlighted by the red dash line shows a single peak continuous with main peak in the implanted section.

Intensity profile was collected by ImageJ [16] software, which includes information of intensity in gray scale and angular position, as shown in Fig.3. The main peak is located at 33" with intensity around 200 and the satellite peak is located at 0" with the intensity of 250. The intensity of the satellite peak is higher than the main peak because the damaged epilayer is thick. The intensity profile can be treated as double axis ω scan. Usually, the curve of double axis ω scan is almost identical with that of double axis ω-2θ scan, so the intensity profile can be assumed to be a ω-2θ rocking curve. The fringes in between the main peak and the satellite peak lie on the lower angular position of the main peak, indicating the crystal is tensile strained. By assuming incident beam as a plane-wave, such intensity profile was fitted manually by RADS simulation software [17]. This program can simulate the rocking curve of multilayers based on composition, thickness, and strain.

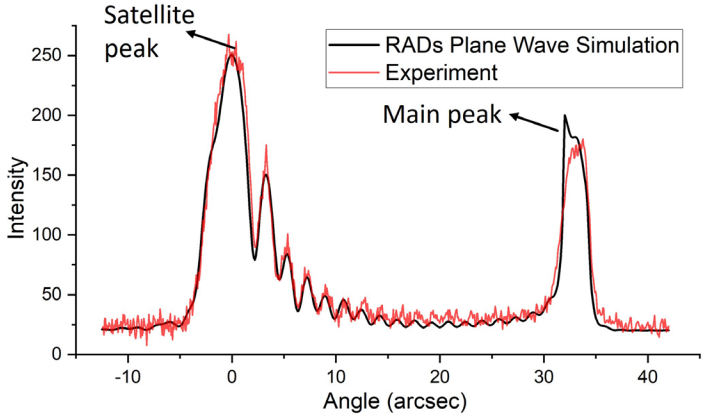

Figure 3. Intensity profile (red) and corresponding RADS plane-wave simulation (black), where the satellite peak (implanted epilayer) is located at 0" and the main peak (substrate/unimplanted epilayer) is located at around 33". Fringes are revealed between the two peaks indicating the presence of a strain gradient in the implanted epilayer.

A strain profile was obtained from RADS simulation shown in Fig. 4(a). It is found that the strain level around 2.3 x 10^{-4} is at the maximum near the surface, then the strain level gently decreases as the depth increases. An abrupt drop of strain level happens at 11.8 μm, and finally the lowest strain around 0.3 x 10^{-4} is indicated at depth of 13 μm. Overall, the strain profile has a box-like shape that is similar to the concentration profile, which indicate that the lattice strain is dominated by the incorporation of the dopant atoms. During the implantation process, the energized ions will penetrate the surface of the wafer. The whole implantation process consists of more than 10 steps, where the acclerated ions in each implant steps will penetrate the surface of the wafer. Therefore, there will be more disordered atoms in the near surface region of the wafer, which will lead to higher tensile strain. On the other hand, only the ions with a higher energy can reach deep into the wafer, the lattice away from the surface suffers less bombardment, resulting in lower tensile strain. Strain map was generated by MATLAB program employed to process the plane-wave topograph data recorded in 0° and 180° positions about the normal of the (0008) plane, where unimplanted region was used as a reference point [4][5]. The strain map shows that overall strain of the wafer is around 1.8 to 2.3 x 10^{-4}, which agrees well with the maximum strain modeled by RADS.

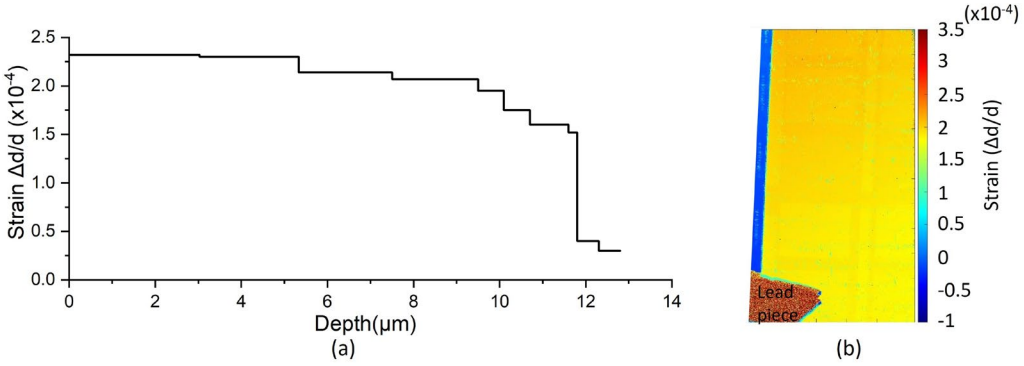

Figure 4. (a) Strain profile for the 12μm thick implanted epilayer obtained from RADS plane wave simulation of recorded X-ray diffracted intensity profile (b) Strain map processed from the SWPXT data recorded in 0° and 180° positions about the normal of the (0008) plane by MATLAB program via using unimplanted region as a reference point. Lead piece at the bottom left corner was used as fiducial mark.

To emphasize the advantages, SXPWT and lab-based diffractometer are compared. Rocking curve obtained using a channel-cut monochromator crystal, Ge (004) (used in Bede D1 diffractometer tool) was simulated by RADS, by assuming the same strain profile as the one obtained from SWPXT. The rocking curve is shown in Fig. 5, where the main peak and satellite peak are located at almost the same position as the RADS plane-wave simulation. Compared to the plane-wave simulation that serves as the rocking curve obtained with both Si(111) monochromator and Si(331) beam conditioner, only the broadened main and satellite peaks are shown in the RADS with Ge (004) and the fine fringes features are not resolved. The Ge (004) monochromator is estimated to provide a probe of 8” width. With such a wide probe, the rocking curve will not have sufficient angular resolution to resolve the individual fringes with separation around 2”. urthermore, compared with synchrotron light source, the intensity of X-ray from a metal target source is relatively low. If the synchrotron experimental setup was equipped in lab-based diffractometer, a low intensity incident beam will be obtained.

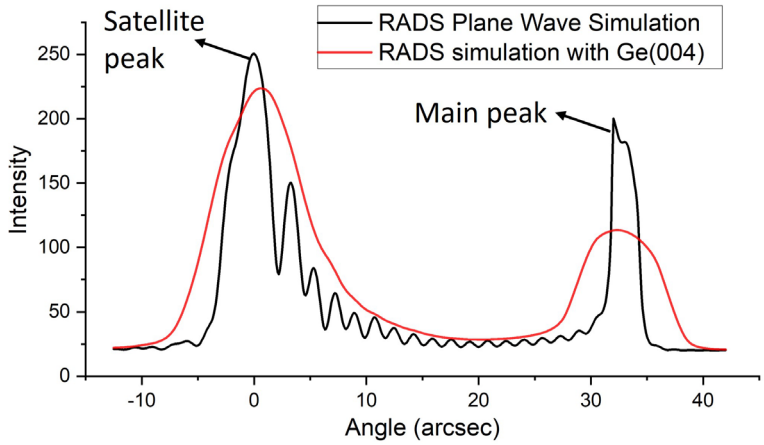

Figure 5. Comparison of RADS simulations of intensity profile from the implanted wafer with same strain profile for plane wave incident beam (black) and incident beam from a metal target source conditioned by a Ge (004) double crystal monochromator (red).

Summary

4H-SiC wafer with 12 μm of epilayer was blanketly multi-step high energy implanted both Al and N atoms at the Tandem Van de Graaff facility at Brookhave National Laboratory. SXPWT and RADS are applied to charaterize the lattice strain in the as-implanted wafer. SXPWT can provide extremely high angular reolusion to reveal fine fringes bettwen the main and satellite peaks. Such patterns are fitted with RADS by assuming incident wave as plane-wave. Strain profile has been obtained, showing maxium strain level of 2.3 x 10^{-4} that correlates with the strain value obtained from strain maps processed by MATLAB program. Moreover, with the same strain profile rocking curve simulated via RADS with Ge (004) can only reveal two broadened main and satellite peaks since the width of the probe is around 8“.

Acknowledgments

Samples provided by GE Research. The information, data, or work presented herein was funded in part by the Advanced Research Projects Agency-Energy (ARPA-E), U.S. Department of Energy, under Award Number DE-AR0001028. The views and opinions of authors expressed herein do not necessarily state or reflect those of the United States Government or any agency thereof.

BNL Work supported by the U.S. Department of Energy, Office of Science, under Contract No. DE[1]SC0012704

This research used resources of the Advanced Photon Source, a U.S. Department of Energy (DOE) Office of Science User Facility operated for the DOE Office of Science by Argonne National Laboratory under Contract No. DE-AC02-06CH11357.

References

[1] J. Guo, Y. Yang, B. Raghothamachar, T. Kim, M. Dudley, J. Kim, J. Cryst. Growth 480 (2017) 119-125.

[2] T. Liu, S. Hu, J. Wang, G. Guo, J. Luo, Y. Wang, J. Guo and Y. Huo, IEEE Access, 7 (2019) 145118-145123.

[3] P. Thieberger, C. Carlson, D. Steski, R. Ghandi, A. Bolotnikov, D. Lilienfeld, P. Losee, Nucl. Instrum. Methods Phys. Res. B: Beam Interact. Mater. At. 442 (2019) 36-40.

[4] J. Guo, Y. Yang, B. Raghothamachar , M. Dudley, S. Stoupin , J. Electron. Mater. 47 (2018) 903- 909.

[5] T. Ailihumaer, Y. Yang, J. Guo, B. Raghothamachar, M. Dudley, J. Electron. Mater., 48 (2019) 3363-3369

[6] R. Ghandi, C. Hitchcock, S. Kennerly, ECS Transactions 104 (2021) 67

[7] R. Ghandi, A. Bolotnikov, S. Kennerly, C. Hitchcock, P.-m. Tang, T.P. Chow, 2020 32nd International Symposium on Power Semiconductor Devices and ICs (ISPSD), IEEE, 2020, 126-129

[8] H. Peng, Z. Chen, Y. Liu, B. Raghothamachar, X. Huang, L. Assoufid and M. Dudley, J. Appl. Crystallogr. 55 (2022) 544-550.

[9] Z. Chen, H. Peng, Y. Liu, Q. Cheng, S. Hu, B. Raghothamachar, M. Dudley, R. Ghandi, S. Kennerly and P. Thieberger, Materials Science Forum 1062, 361-365

[10] Z. Chen, Y. Liu, H. Peng, T. Ailihumaer, Q. Cheng, S. Hu, B. Raghothamachar, M. Dudley, ECS Transactions 104 (2021) 75

[11] Y. Liu, H. Peng, Z. Chen, T. Ailihumaer, Q. Cheng, S. Hu, B. Raghothamachar, M. Dudley, , ECS Transactions 104(7) (2021) 113.

[12] K. Wieteska, W. Wierzchowski, W. Graeff, A. Turos, R. Grötzschel, Journal of Synchrotron Radiation 7(5) (2000) 318-325

[13] W. Wierzchowski, K. Wieteska, W. Graeff, A. Turos, Journal of alloys and compounds 286 (1999) 343-348

[14] W. Wierzchowski, A. Turos, K. Wieteska, A. Stonert, R. Ratajczak, P. Jóźwik, R. Wilhelm, S. Akhamadaliev, K. Mazur, C. Paulmann, X-Ray Spectrometry 44 (2015) 371-378

[15] W.H. Zachariasen, Theory of X-ray diffraction in crystals, Dover Publications, INC.1945.

[16] C.A. Schneider, W.S. Rasband, K.W. Eliceiri, NIH Image to ImageJ: 25 years of image analysis, Nature methods 9 (2012) 671-675

[17] M. Wormington, C. Panaccione, K. M. Matney, and K. D. Bowen, Phil. Trans. R. Soc. Lond. A 357 (1999) 2827-2848.